JOURNAL OF MATERIALS SCIENCE **34** (1999) 4775–4781

The effect of graphite flake morphology on the thermal diffusivity of gray cast irons used for automotive brake discs

R. L. HECHT
Vehicle Safety Research Department, Ford Research Laboratory, Dearborn, MI 48121-2053
E-mail: rhecht@ford.com

R. B. DINWIDDIE, H. WANG
High Temperature Materials Laboratory, Oak Ridge National Lab, Oak Ridge, TN 37831

Thermal diffusivity of automotive grade SAE G3000 (d) gray cast iron has been measured as a function of graphite flake morphology, chemical composition and temperature. Cast iron samples used for this investigation were cut from "step block" castings designed to produce iron with different graphite flake morphologies resulting from different cooling rates. Samples were also machined from prototype and commercial brake rotors, as well as from a series of cast iron slugs with slightly varying compositions. Thermal diffusivity was measured at room and elevated temperatures via the flash technique. Graphite flake morphology of the various cast iron samples was quantified stereologically with image analysis techniques. Several geometric features of the graphite flake morphology were quantified. It was found that the thermal diffusivity of these gray cast irons increases with carbon equivalent and has a strong linear correlation to graphite flake length. For gray iron with the same chemical composition, a four fold increase in the graphite flake size results in a 50% increase in thermal diffusivity. Amongst the commercial rotors, room temperature thermal diffusivity varied from 0.156 to 0.200 cm^2/s.

1. Introduction

Gray cast iron has been the primary material for automotive brake rotors (discs) because of its excellent thermal transport ability and its damping properties. A brake rotor must be able to dissipate the frictional heat generated by application of the brake pads during a stop. One way to improve the heat transfer ability of a rotor is to increase the material's thermal diffusivity. Thermal diffusivity describes the rate of heat propagation during transient processes, and so is a fundamental material parameter for the design of brakes. Thermal diffusivity can be used to calculate thermal conductivity, the steady-state measure of how a material transmits heat. Gray cast iron rotors with improved thermal conductivity have shown increased resistance to heat cracks [1], possibly improving the service life of the brake. If the thermal transport ability of gray cast iron can be increased without sacrificing other design criteria, brake performance may be enhanced.

Graphite inclusions have a significantly higher thermal diffusivity than the matrices of cast irons. Distribution of the graphite phase is the primary influence on thermal transport. Nodular iron, where graphite is in spherical form, exhibits lower conductivity than compacted graphite, which in turn has a lower conductivity than gray iron with its flake graphite; as graphite flakes get longer, diffusivity and conductivity increase [2–5]. The phase of the cast iron matrix influences diffusivity a small degree, and ferrite has a higher diffusivity value than pearlite [3, 4].

Most rotors on production passenger cars today are gray cast iron with Type A or B graphite flakes (AFS-ASTM A247 designation) embedded in a pearlite matrix. However, there are variations in chemical composition and processing between foundries which lead to microstructural differences between rotors produced to the same specification. Solidification rate impacts graphite flake morphology, hence different casting mold configurations (e.g. number of parts/mold) or new component designs may result in slightly different graphit flake morphologies. Knowing how morphology impacts thermal transport allows assessment of how a variation in disc production will impact thermal management in the rotor.

Thermal diffusivity was measured at room and elevated temperatures for pearlitic gray cast irons to determine whether subtle differences in morphology alter heat transfer. In order to isolate the effects of graphite flake shape from the influences of composition, test specimens were made from "step block" castings designed to have 5 different cooling rates and hence different graphite flake morphologies in each step. Steps are labeled 1–5, with Step 1 being the thinnest step with the fastest cooling. Variations in chemical composition

were considered by cutting material specimens from production and prototype ventilated front rotors of similar dimensions, labeled here US #1, US #2, US #3, German, Japanese, Prototype US and Prototype Europe. In order to isolate the influences of composition, 8 cast iron alloys with slight compositional variations, were cast in a large cylindrical mold. Test specimens were cut from these castings designated as Alloys 1–8.

2. Experimental

Room temperature thermal diffusivity was measured by the flash technique [6] using a xenon flash system at the High Temperature Materials Laboratory at Oak Ridge National Laboratory. To perform this measurement, one face of a sample of known thickness is subjected to an intense, brief heat pulse, and the time for the pulse to propagate to the opposite face of the sample is recorded. The diffusivity, α, is calculated from the time it takes for the rear surface to achieve $1/2$ of its maximum temperature rise,

$$\alpha = C D^2 / t_{0.5} \tag{1}$$

where C is a dimensionless parameter, D is the specimen thickness, and $t_{0.5}$ is the half rise time of the rear surface temperature. Analysis software determines the value of C using Koski's parameter estimation technique [7] applied to Clark and Taylor analysis [8]. Clark and Taylor's analysis includes the effect of radiation heat losses.

Specimens used for the diffusivity measurements are disk-shaped, nominally 12.7 mm in diameter and 3.18 mm thick. Before testing, each specimen was measured and weighed to determine its density and thickness, and coated with carbon to maximize the energy absorption. Five diffusivity measurements of each specimen were made at room temperature; between 3 and 8 specimens were tested for each alloy and each test condition, assuring a statistically reliable and representative value for each sample and for each alloy.

The elevated temperature thermal diffusivity was measured on a system equipped with a moveable Nd:glass laser, a cryogenically cooled InSb IR detector, and four furnaces [9]. A low temperature aluminum block furnace was used to achieve the test temperatures of 200°–500 °C. Oxidation of the cast iron samples was minimized by flowing ultra high purity argon through the furnace. Each specimen was measured three times at each elevated temperature. The Koski parameter estimation technique applied to Cowen's analysis [10] was used to determine the value of C in Equation 1 and to generate the diffusivity results for the elevated temperature results.

Automotive disc brakes operate at high temperatures and are subject to the influences of environment. Another goal of this work was to determine how the presence of oxide scale effects thermal diffusivity. Rotor samples were oxidized in a furnace at 500 °C for 1, 10 and 270 h. Thermal diffusivity was subsequently measured at room temperature.

To quantify the graphite flake morphology, diffusivity specimens were mounted and prepared by standard metallography, avoiding the use of wet grinding to prevent graphite flake pullout. Metallographic mounts were observed by optical microscopy in an unetched condition. Image analysis was performed with a Nikon optical microscope and Image Pro Plus software to quantify the structure, size and shape of the graphite flakes. Chemical composition of each cast iron alloy was determined on a JOEL optical emission spectrometer (OES), and LECO combustometric analysis was used to determine the weight percents of C and S.

3. Results and discussion

The chemical composition in wt % of the alloys appears in Table I. Fig. 1 shows that for the rotor and cast iron alloy samples there is a positive, almost linear dependence of thermal diffusivity with increasing carbon equivalent (CE), where CE = % C + 1/3(% Si+ % P). This increase is expected since increasing the % C or CE is the most direct way to improve the graphitization in gray iron. Amongst the brake rotor samples, there is a 25% increase in diffusivity with a 0.4% increase in CE. The general linear trend seen in part of Fig. 1 extends beyond the carbon % range of the rotors studied here (3.43–3.79% C) to 2.5–4.0% C [1]. Other research has demonstrated the effect of increasing thermal diffusivity with increasing % CE from 3.6 to 4.8% CE [11].

In order to isolate the effect on thermal diffusivity of the graphite shape from the composition (or CE), "step block" castings were produced to gray iron G3000 specification. A step block casting is shaped like a staircase; step heights were 3.175, 6.35, 12.7, 25.4, and 50.8 mm, with each step being 124 mm wide and 56 mm deep. Because of the difference in step thickness, each step experiences a different solidification and cooling rate, producing different graphite flake morphologies in material with the same composition. Although all of the rotor and alloy samples have a fully pearlitic microstructure with only trace amounts of ferrite, the step block castings contain small amounts of ferrite in the primarily pearlitic matrix. The thinnest step, Step 1, contains approximately 4.9 vol % ferrite, Step 2 contains 3.8 vol %, and the amount of ferrite drops to a minimum in Step 5 of 0.4 vol % ferrite.

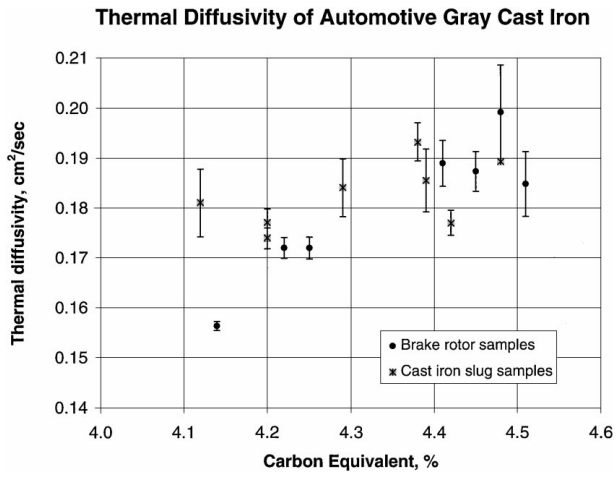

Figure 1 Room temperature thermal diffusivity increases as a function of carbon equivalent (CE). Error bars are ± one standard deviation.

TABLE I Chemical compositions (wt %)

	Rotors								Cast iron alloys							
	Japanese	German	US #1	US #2	US #3	Proto. Europe	Proto. US	Step blocks	Alloy 1	Alloy 2	Alloy 3	Alloy 4	Alloy 5	Alloy 6	Alloy 7	Alloy 8
Carbon	3.69	3.79	3.51	3.45	3.43	3.78	3.79	3.64	3.39	3.42	3.40	3.61	3.60	3.63	3.50	3.70
Manganese	0.56	0.74	0.88	0.65	0.71	0.59	0.51	0.68	0.65	0.71	0.84	0.83	0.67	0.70	0.89	0.89
Phosphorus	0.03	0.05	0.01	0.02	0.03	0.03	0.04	0.05	0.09	0.11	0.10	0.09	0.08	0.10	0.11	0.11
Sulfur	0.10	0.09	0.10	0.08	0.13	0.10	0.16	0.01	0.12	0.12	0.12	0.12	0.13	0.12	0.12	0.15
Silicon	2.14	2.01	1.87	2.30	2.43	2.16	1.90	2.20	2.12	2.26	2.33	2.23	2.30	2.28	2.26	2.25
Copper	0.05	0.19	0.95	0.10	0.28	0.08	1.20	0.10	0.27	0.29	0.29	0.31	0.33	0.29	0.18	0.20
Nickel	0.03	0.10	0.01	0.08	0.12	0.08	0.07	0.01	0.13	0.13	0.13	0.13	0.13	0.12	0.12	0.12
Chromium	0.05	0.12	0.24	0.30	0.31	0.25	0.14	0.31	0.21	0.40	0.39	0.22	0.37	0.20	0.19	0.43
Iron	Base	Base	Base	Base	Base	Base	Base	Base	Base	Base	Base	Base	Base	Base	Base	Base
Carbon Equivalent	4.41	4.48	4.14	4.22	4.25	4.51	4.44	4.39	4.12	4.20	4.20	4.38	4.39	4.42	4.29	4.48

TABLE II Microstructural characteristics of gray cast iron diffusivity specimens

Sample	Average flake length (mm)	Maximum flake length (mm)	Surface/Volume (1/mm)	Aspect ratio	Fields of view analyzed	ASTM	
						Flake type	Size class
Step 1 (3.18 mm)	14	195	0.88	2.6	27	D, A	3–4
Step 2 (6.35 mm)	42	383	0.45	4.4	20	A	2
Step 3 (12.7 mm)	58	556	0.40	6.2	20	A	2
Step 4 (25.4 mm)	89	685	0.37	5.4	19	A	1
Step 5 (50.8 mm)	94	881	0.19	6.5	10	A	1
German	47	547	0.39	3.2	10	A, B	2
Japanese	71	710	0.34	4.8	10	A	1
Proto. Europe	43	575	0.41	3.1	20	A, B	2
Proto. US	52	655	0.44	4.4	20	A	1–2
US #1	51	403	0.32	3.8	10	A	2
US #2	46	469	0.38	3.1	10	A	2
US #3	49	564	0.39	3.5	20	A	2

Commercial image analysis software was used to measure the graphite flake morphology parameters such as flake length, area, major shape axis, minor shape axis and shape perimeter on unetched mounts. These parameters are defined in the schematic pictured in Fig. 2. Table II lists average microstructural characteristics of the graphite found in each step and in the brake rotors. The "Average Flake Length" is simply the average value L from all the flakes measured for a particular iron over all the fields of view. The "Maximum Flake Length" is the maximum value of L observed for a particular iron over the all the fields of view. It should be noted that only flakes fully visible in the field of view were measured and tabulated as is necessary for accurate assessment of average length values. A three dimensional property important for heat transfer is surface area/volume; in order to estimate this property for the graphite from two dimensional images, the average graphite shape perimeter, P was divided by the area enclosed, A, and this value is included in Table II as "Surface/Volume." The "Aspect Ratio" was defined as major axis/minor axis or X/Y.

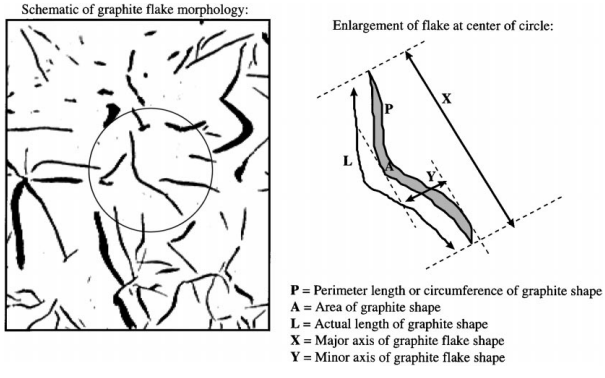

Figure 2 This schematic shows how the parameters used to characterize graphite flake morphology are defined. A commercial image analysis software program was used to measure the dimensions defined here: P, A, L, X, and Y, for thousands of flakes in each diffusivity sample.

Examples of unetched optical images used for measuring graphite parameters are shown in Fig. 3. Actual diffusivity samples were mounted, polished and used for the microstructural measurements, hence the number of fields of view analyzed was limited by the size of the samples. The number of fields of view analyzed for each sample type is listed in Table II; this corresponds to measuring between 5000 and 12000 flakes. Alloys 1–8 were not used in the microstructural study because they were all cast in the same large cylindrical mold which resulted in very large flake sizes, e.g. maximum flake lengths of 1000–1400 μm. With such large flakes sizes statistically valid assessment of the graphite morphology was not possible on the small diffusivity samples.

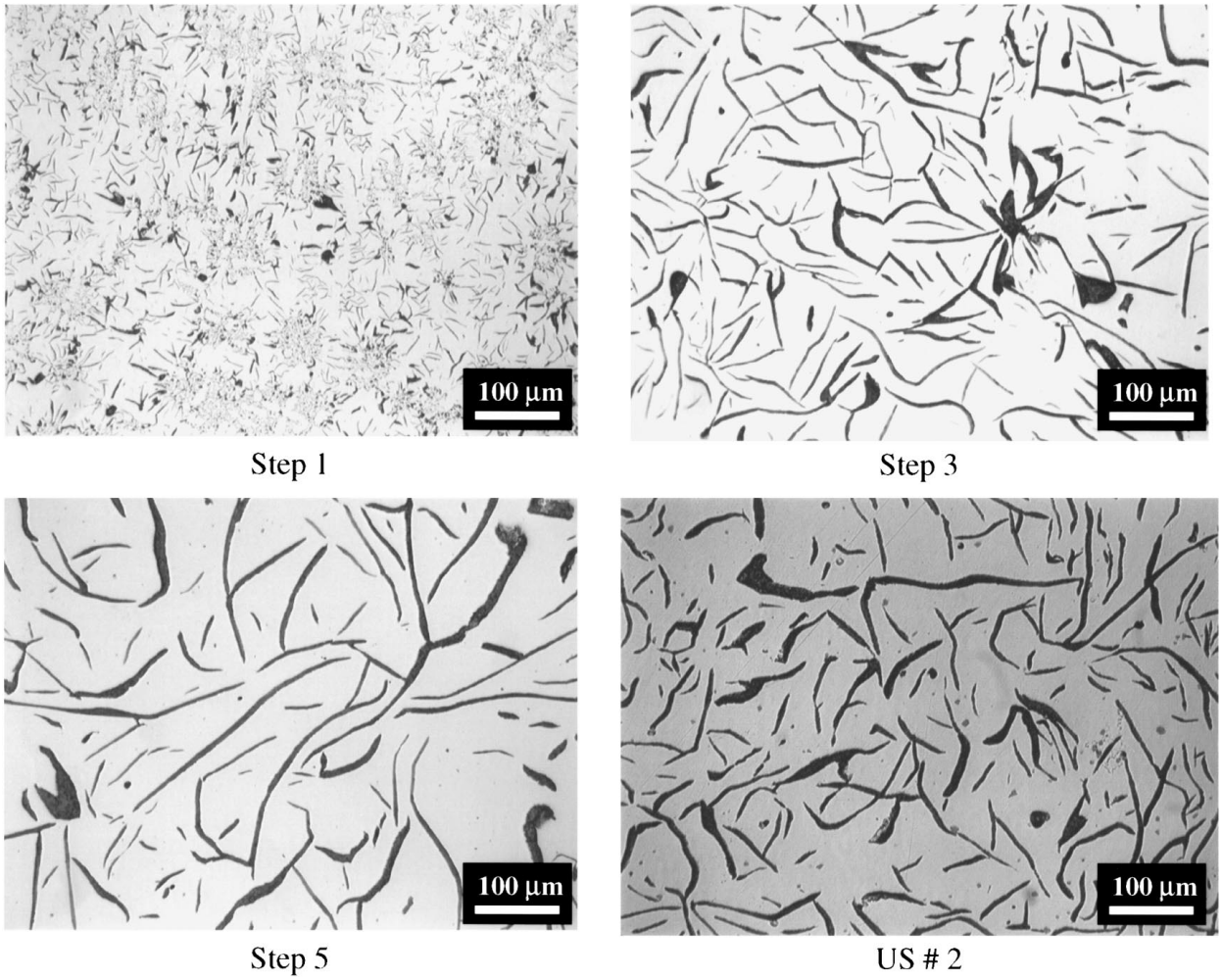

Figure 3 Optical images of gray iron from Step 1, Step 3, Step 5 and US #2. Step 1 contains Type D and Type A graphite; other samples have only Type A graphite flakes.

The average flake length-diffusivity relationship is shown in Fig. 4a, and maximum observed flake length vs. diffusivity is plotted in Fig. 4b. In Fig. 4, the diffusivity value of a particular sample is plotted against the flake parameter measured on that same sample. For the step blocks it was found that both the average flake length and the maximum flake length exhibited a virtually linear relationship with diffusivity; longer flakes result in greater diffusivity. For the step blocks, a linear correlation of diffusivity and average graphite flake length has an R^2 value of 0.90 (Fig. 4a) while the linear fit with maximum flake length was not as good, with $R^2 = 0.71$ (Fig. 4b). Considering Fig. 4 and the data in Table II, the presence of Type D (interdendritic) graphite, as well as the shorter Type A flake size in Step 1, drastically reduced thermal diffusivity in those samples. Although the matrix also contributes to diffusivity, and ferrite is a better heat conductor than lamellar pearlite, the small amount of free ferrite present in Steps 1 and 2 is not enough to compensate for the lower diffusivity resulting from the interdendritic graphite and shorter Type A flakes.

Diffusivity specimens from each rotor were analyzed to determine if the graphite flake length also accounts for the variation found in the rotors' diffusivity. For the rotor samples, maximum flake length showed a stronger agreement with the step blocks than the average flake length, as seen in Fig. 4. The step block specimens, which all come from the same casting, illustrate the graphite length effect clearly because compositional influences are reduced. The rotors vary in composition but still show a strong trend of increasing diffusivity with maximum flake length. For gray irons with a similar flake size, CE is a better predictor of diffusivity. (Flake size does not necessarily increase with increasing CE.) Consistent with the diffusivity-length relationship, it was also noted that as the aspect ratio of the graphite flakes increases, thermal diffusivity increases. Fig. 5 shows this remarkably linear relationship for the step block samples ($R^2 = 0.99$), and again the rotor diffusivity values appear to be influenced by more than just graphite shape, and do not neatly follow the linear increase.

Figs 4 and 5 confirm that the length and shape of the graphite effects heat transport. Graphite in gray iron is an interconnected three-dimensional network; what is known as a "graphite flake" in a two dimensional metallographic image is a curved basal section through the crystal or an edge-on view of the basal planes [12]. The thermal transport ability of graphite in the basal plane significantly exceeds its value along the *C*-axis. Thermal conductivity along the *C*-axis is approximately 84 W/mK but along the basal plane is 293–419 W/mK [12]. A gray iron alloy with longer

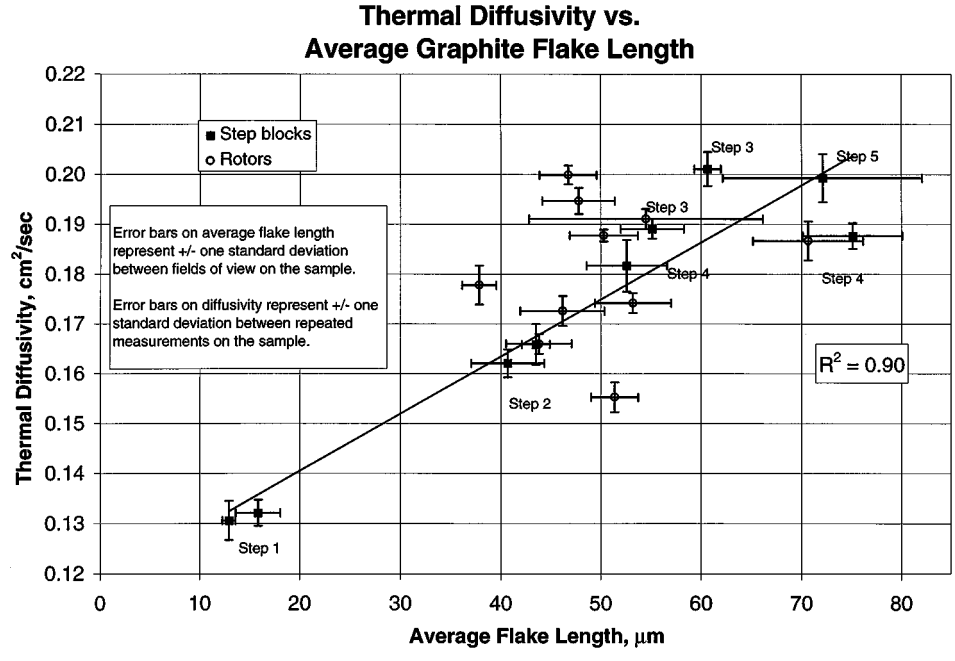

(a)

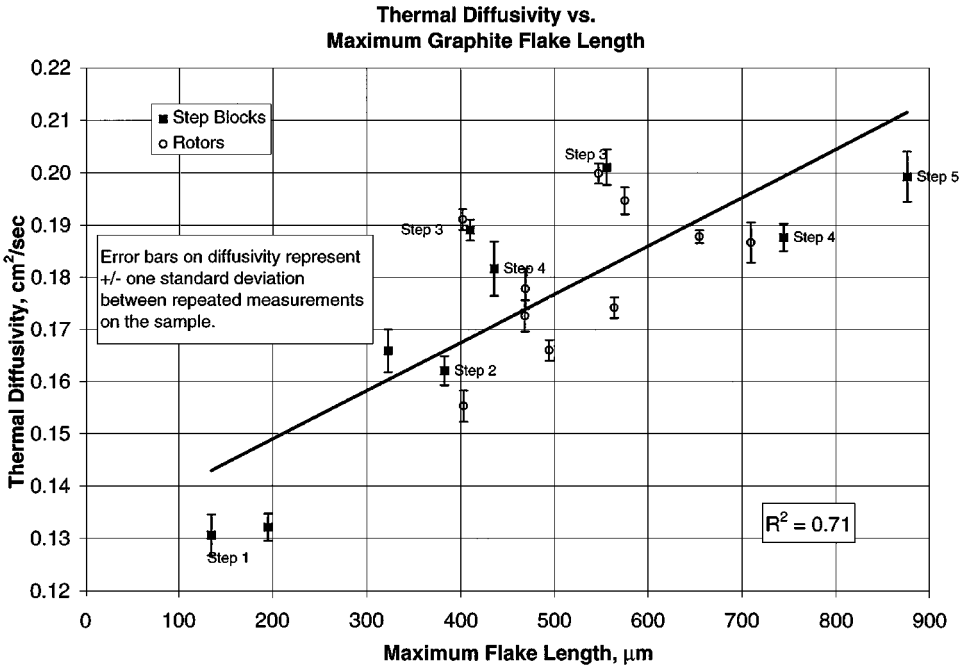

(b)

Figure 4 (a) The average flake length measured on step block and rotor samples exhibits an increasing relationship with the room temperature thermal diffusivity. Line is a fit through the step block sample results only. (b) For both the step blocks and the rotor samples, room temperature thermal diffusivity increased as the maximum observed graphite flake length increased. Linear correlation shown is for step block samples only.

(or higher aspect ratio) flakes therefore has more of the basal planes available for heat flow, and hence that cast iron will exhibit a higher diffusivity (and thermal conductivity).

Cast iron slug samples (Alloys 1–8) all had average flake lengths of 80–100 μm, and maximum flake lengths of 1000–1400 μm due to the drastically slower cooling rate in this mold configuration compared to the cooling rate in the commercial rotors. However, these gray irons did not follow the trends observed in Figs 4 and 5. Diffusivity values were comparable to the commercial rotors (Fig. 1.) even through the flakes were longer. This suggests that either there is a limit to how much the diffusivity can be improved by increased flake length or that other factors limited the diffusivity of the gray iron from these large castings. It should be noted that these castings contained significant porosity which would reduce diffusivity. The large volume of the mold (a cylinder with approximately 160 mm diameter and 300 mm height) means that significant segregation could occur during solidification. Chemical analysis was not performed on the same samples that were used to measure diffusivity, hence the average compositions listed in Table I might vary for individual samples. Another possible cause for the discrepancy relates to oxidation; oxidation can occur along the graphite-pearlite interfaces and longer flakes mean that oxidation could reach greater depth below the surface.

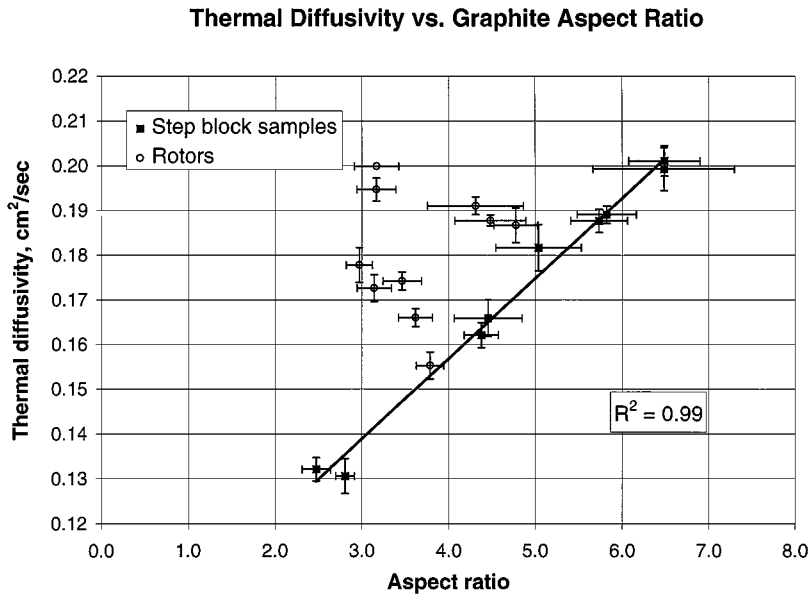

Figure 5 For the step block samples, room temperature thermal diffusivity increased linearly with graphite flake aspect ratio; this relationship did not exist for the rotor samples. Error bars represent ± one standard deviation as in previous figures.

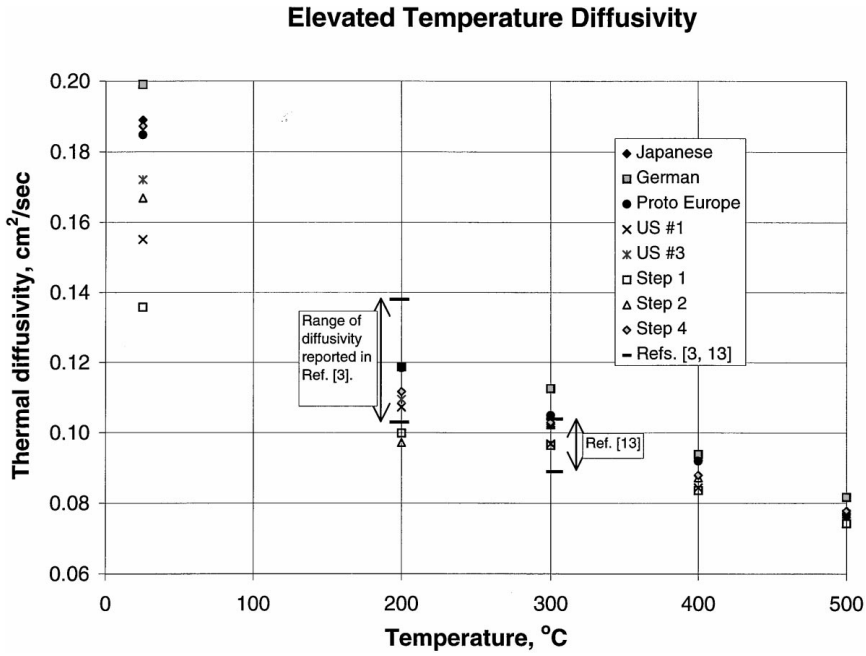

Figure 6 Thermal diffusivity of gray cast iron decreases with temperature. The difference in thermal diffusivity between gray iron variations diminishes at elevated temperature.

At this time, it is not clear why the graphite structure analysis for these gray irons is not consistent with the other data.

Elevated temperature diffusivity was measured by a laser flash system at temperatures between 200° to 500 °C for Steps 1–4 and several of the cast iron rotors. Diffusivity decreases with temperature as shown in Fig. 6, where the average diffusivity value for each temperature is plotted for several gray irons. Gray iron's ability to transport heat decreases as its temperature increases. Fig. 6 shows that the difference in diffusivity for different cast irons is less significant at elevated temperatures. The results agree reasonably well with elevated temperature diffusivity values reported for "coarse flake" gray iron from 200°–700 °C [3]. Data at 200 °C reported in Ref. 3 is included on Fig. 6, along with results from Ref. 13, whose authors measured diffusivity at 300 °C.

Since brake rotors operate in a corrosive environment and at high temperatures, the effects of oxide scale on the diffusivity were investigated. Room temperature thermal diffusivity dropped following 270 h of exposure to 500 °C, as shown in Fig. 7. Insignificant changes in the pearlitic matrix would be expected following so short an exposure at 500 °C, and the graphite flake morphology would not be affected at all. This diffusivity change can be attributed to the growth of oxide scale on the sample surfaces. The largest influence was observed in the German rotor specimen which experienced a 14% drop in diffusivity. Although there was no measurable weight gain to quantify the amount of scale developed it was visible on the sample surfaces. The German rotor

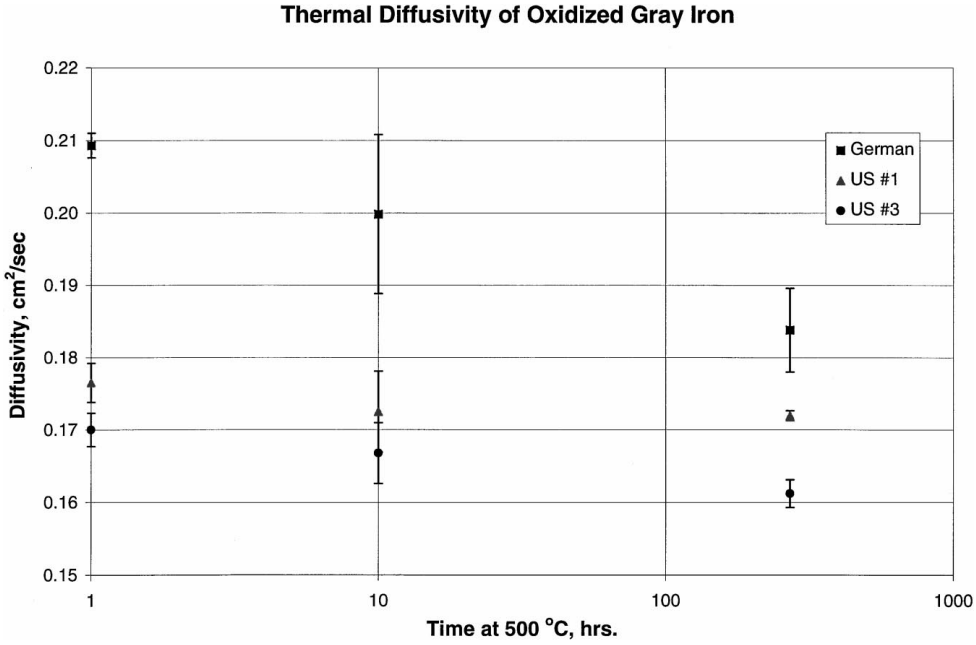

Figure 7 Room temperature thermal diffusivity of gray irons dropped with increasing exposure to 500 °C. Error bars represent ± one standard deviation.

samples have greater flake sizes than the other samples and therefore may be more vulnerable to deeper oxide intrusion. Results in Fig. 7 suggest that if oxidation occurs while in service gray iron brake rotors may experience a significant drop in their heat transport ability.

4. Conclusions

It was shown that thermal diffusivity is influenced by changes in chemical composition of gray cast iron, and that a roughly linearly increasing relationship exists between room temperature diffusivity and carbon equivalent (CE) within the carbon range of gray cast iron. Figs 4 and 5 show that graphite flake morphology and geometry affect diffusivity in G3000 standard automotive gray iron. For a constant CE, as in the step block castings, average flake length, maximum flake length and aspect ratio for Type A graphite flakes show a strong linear correlation with thermal diffusivity; the longer the flakes the greater the diffusivity. For the composition range within the rotors tested, maximum flake length proved to be a reasonable indicator of diffusivity. Diffusivity decreases in gray cast irons as the temperature increases up to 500 °C. At elevated temperatures, the difference in diffusivity observed between alloys decreased, and the materials had similar values at 500 °C. These data suggest that higher diffusivities and thermal benefits may be achieved through control of the casting process to produce gray cast iron rotors with long Type A graphite flakes for a particular alloy composition.

Acknowledgement

Research partially sponsored by the Assistant Secretary for Energy Efficiency and Renewable Energy, Office of Transportation Technologies, as part of the High Temperature Materials Laboratory User Program, Oak Ridge National Laboratory, managed by Lockheed Martin Energy Research Corp. for the US Department of Energy under contract number DE-AC05-96OR22464.

References

1. Y. JIMBO, T. MIBE, K. AKIYAMA, H. MATSUI, M. YOSHIDA and A. OZAWA, *SAE International* **SAE 900002** (1990) 22.
2. K. B. PALMER, *J. BCIRA* **8**(540) (1960) 266.
3. J. OMEROD, R. E. TAYLOR and R. J. EDWARDS, *Met. Tech.* April (1978) 109.
4. D. FITZGEORGE and J. A. POPE, *Transactions of the North East Coast Institution of Engineers and Shipbuilders* **75** (1959) 284.
5. R. L. HECHT, R. B. DINWIDDIE, W. PORTER and H. WANG, SAE Technical Paper Series 962126 (1996).
6. W. J. PARKER, R. J. JENKINS, C. P. BUTLER and G. L. ABBOTT, *J. Appl. Phys.* **32** (1961) 1679.
7. J. A. KOSKI, in Proceedings of the 8th Symposium of Thermophysical Properties, Gaithersburg, MD, June 1981 (ASME, New York, 1981) Vol. 2, p. 94.
8. L. M. CLARK and R. E. TAYLOR, *J. Appl. Phys.* **46** (1975) 714.
9. H. WANG, R. B. DINWIDDIE and P. S. GAAL, in "Thermal Conductivity 23," edited by K. E. Wilkes *et al.* (Technomic Publishing Co., Lancaster, PA, 1996) p. 119.
10. R. D. COWAN, *J. Appl. Phys.* **34** (1963) 926.
11. S. YAMADA and T. KURIKUMA, Paper F98T683, Proceedings from 1998 FISITA World Automotive Congress, Paris, September–October 1998.
12. H. T. ANGUS, "Cast Iron: Physical and Engineering Properties," (Butterworths, London, 1976) p. 126.
13. P. FERDANI, R. A. EMMETT and J. D. HOLME, Paper 25, Leading Through Innovation T&N Symposium, Wurzburg, Indianapolis, 1995.

Received 19 February 1998
and accepted 23 March 1999